INTERFACE

rsif.royalsocietypublishing.org

Report

Cite this article: Pete AE, Kress D, Dimitrov MA, Lentink D. 2015 The role of passive avian head stabilization in flapping flight. *J. R. Soc. Interface* **12**: 20150508.
http://dx.doi.org/10.1098/rsif.2015.0508

Received: 6 June 2015
Accepted: 4 August 2015

Subject Areas:
biomechanics, biomimetics

Keywords:
head stabilization, flapping, flight, avian, neck, gust

Author for correspondence:
David Lentink
e-mail: dlentink@stanford.edu

Electronic supplementary material is available at http://dx.doi.org/10.1098/rsif.2015.0508 or via http://rsif.royalsocietypublishing.org.

THE ROYAL SOCIETY PUBLISHING

The role of passive avian head stabilization in flapping flight

Ashley E. Pete, Daniel Kress, Marina A. Dimitrov and David Lentink

Department of Mechanical Engineering, Stanford University, Stanford, CA, USA

Birds improve vision by stabilizing head position relative to their surroundings, while their body is forced up and down during flapping flight. Stabilization is facilitated by compensatory motion of the sophisticated avian head–neck system. While relative head motion has been studied in stationary and walking birds, little is known about how birds accomplish head stabilization during flapping flight. To unravel this, we approximate the avian neck with a linear mass–spring–damper system for vertical displacements, analogous to proven head stabilization models for walking humans. We corroborate the model's dimensionless natural frequency and damping ratios from high-speed video recordings of whooper swans (*Cygnus cygnus*) flying over a lake. The data show that flap-induced body oscillations can be passively attenuated through the neck. We find that the passive model robustly attenuates large body oscillations, even in response to head mass and gust perturbations. Our proof of principle shows that bird-inspired drones with flapping wings could record better images with a swan-inspired passive camera suspension.

1. Introduction

Typical for flying animals, image stabilization is critical for birds to navigate airspace and control their flight path [1,2]. Without it, birds would experience shaky vision and have difficulty holding their gaze on close-range objects used to control flight like flock mates and obstacles [3]. Image stabilization is accomplished through head and eye coordination in concert with neural processing, a process that is poorly understood in avian flight [4]. One behaviour fundamental to avian image stabilization is the ability of birds to stabilize their head with respect to the horizon. Head stabilization may be observed by eye in long-necked birds, such as swans or geese, whose necks make large compensatory motions to attenuate the oscillatory displacement of the body with each wingbeat. Geese in particular are known for performing a remarkable whiffling manoeuvre during landing in which they keep their head fixed horizontally, while briefly rolling their body 180° to fly inverted [5]. This contrast between continuous beat-by-beat head stabilization and stabilization during occasional complex manoeuvres raises questions about the role of high-level versus low-level neural control for the sake of economy. Avian head and body stabilization behaviours have previously been studied in birds sitting on perches that were forced to oscillate vertically [6], and in sitting birds undergoing flow-stimulation directed at the breast [7]. Flight experiments such as those by Erichsen *et al*. [8] reported head orientation, but not positions of the head and body, whereas others consider rotational rather than translational stability [7]. Vertical head stabilization is best understood in humans [9,10]. Remarkably, humans rely on passive head stabilization during characteristic gaits such as walking and running over even terrain [11,12], analogous to flight in a calm atmosphere. Passive stabilization can be interpreted as minimal modulation of the muscle stiffness and damping constants so they interact with the system's mass in such a way that their passive dynamics compensate for periodic disturbances such as strides or wingbeats. To gain insight into the potential role of passive head stabilization in avian flight, we corroborated the head-to-body transfer function of the whooper swan *Cygnus cygnus* from high-speed videos of flight over a lake. To determine whether passive head stabilization also works in a gust, we simulated it using the corroborated whooper swan neck model.

2. Neck transfer function of a whooper swan

We tracked the eye and neck vertex (visible juncture of neck and breast) points from high-speed videos (Phantom HD Gold camera at 240–288 frames s^{-1}) of imprinted whooper swans in steady flight over a lake, courtesy of www.birdsinslowmotion.com (figure 1*a*; electronic supplementary material, video S1). We selected five level flights of unidentified individuals from which we could extract low-noise motion data (data available at public repository: http://purl.stanford.edu/pw311wn7849), using tracking software developed by Hedrick [13]. The single camera perspective enabled us to extract relative displacements of the head and body projected on the image plane (figure 1*a*). Because the oscillatory displacement due to flapping is principally vertical, we use the vertical projection of relative displacement (figure 1*c*,*d*; electronic supplementary material, figures S1 and S2). To determine whether the transfer function of the neck can be represented by a passive mass–spring–damper system (figure 1*b*), we analyse relative head and body displacements. The fraction of the body displacement that is transferred to the head is quantified by the gain of the (steady-state) transfer function:

$$|G(\omega)| = \left|\frac{\Delta_{\text{head}}}{\Delta_{\text{body}}}\right| = \frac{\sqrt{1+(2\zeta\omega/\omega_n)^2}}{\sqrt{(1-(\omega/\omega_n)^2)^2+(2\zeta\omega/\omega_n)^2}}. \quad (2.1)$$

The offset between the head response and body input at equivalent amplitude ratios of displacement is quantified by the phase of the (steady-state) transfer function:

$$\angle G(\omega) = \angle\Delta_{\text{head}} - \angle\Delta_{\text{body}} = \arctan(2\zeta\omega/\omega_n) - \arctan\left(\frac{2\zeta\omega/\omega_n}{1-(\omega/\omega_n)^2}\right). \quad (2.2)$$

In which $(\angle)\Delta_{\text{head}}$ and $(\angle)\Delta_{\text{body}}$ are the relative head and body displacements (and phase angles), respectively, $\zeta = c/2\sqrt{km}$ is the non-dimensional damping ratio of the neck (with c, damping constant; k, spring constant; m, head mass), and ω/ω_n is the ratio of forcing frequency to the natural frequency of the neck, $\sqrt{k/m}$. This simple model ignores the complexity of the neck in a similar manner as the commonly accepted pogo stick model that represents terrestrial locomotion [14] and is analogous to the one that predicts head stabilization in walking humans at the stride frequency [11]. The musculoskeletal neck system of birds is, however, arguably more complex with about three times the vertebrae mammals have and 200 muscles on each side, which enables fast head motion [2,15]. To determine how well our passive model predicts head stabilization in whooper swans, we determined the damping and natural frequency ratios that best represent the neck's transfer function during each of the five flights. For this, we first removed low-frequency altitude and camera pan and tilt variations, using MATLAB's Loess smoother with a span of two wingbeats to high-pass filter the traces (HP in figure 1*d*,*e*). Subsequently, we determined the gain (head-to-body amplitude ratio based on local extrema) and phase (cross-correlation of the entire trace), figure 1*f*. The data show that the average head gain is four times lower than the body's, the head is thus stabilized. The phase difference between neck and body is close to 180°, or half a wingbeat period, and thus tuned for compensating body motion. Using these data, we numerically determined which $\omega_n/\omega_{\text{flap}}$

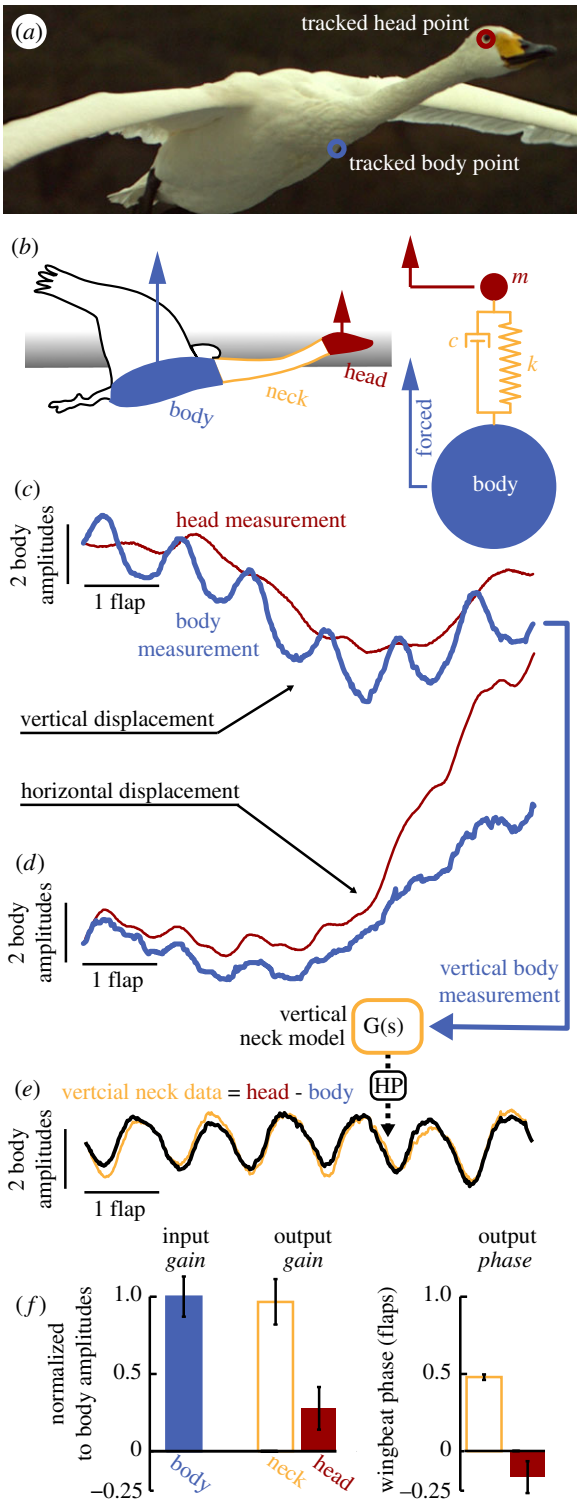

Figure 1. A mass–spring–damper model predicts passive head stabilization in whooper swans. (*a*) The cropped video frame illustrates the tracked points used to reconstruct vertical head and body displacements. (*b*) The neck model stabilizes the motion of the head with mass, m, using a vertical spring with stiffness, k and damping constant, c. (*c*) Raw traces of the vertical displacement for the head and body of a whooper swan in the high-speed video. The vertical axis shows body displacement divided by average body amplitude, while the horizontal axis shows time divided by flap period. (*d*) Raw traces of the horizontal displacement for the head and body, using the same units as in (*c*), show that oscillatory displacement due to flapping is principally vertical. (*e*) High-pass filtered (HP) head and body traces are used to corroborate the neck transfer function that minimizes r.m.s.e. (yellow, measured; black, predicted). (*f*) Gain and phase of body, neck and head. Error bars indicate the standard deviation between flights. The body and neck have the same gain with opposite phase, which shows that the neck compensates for body motion; $n = 5$ flights.

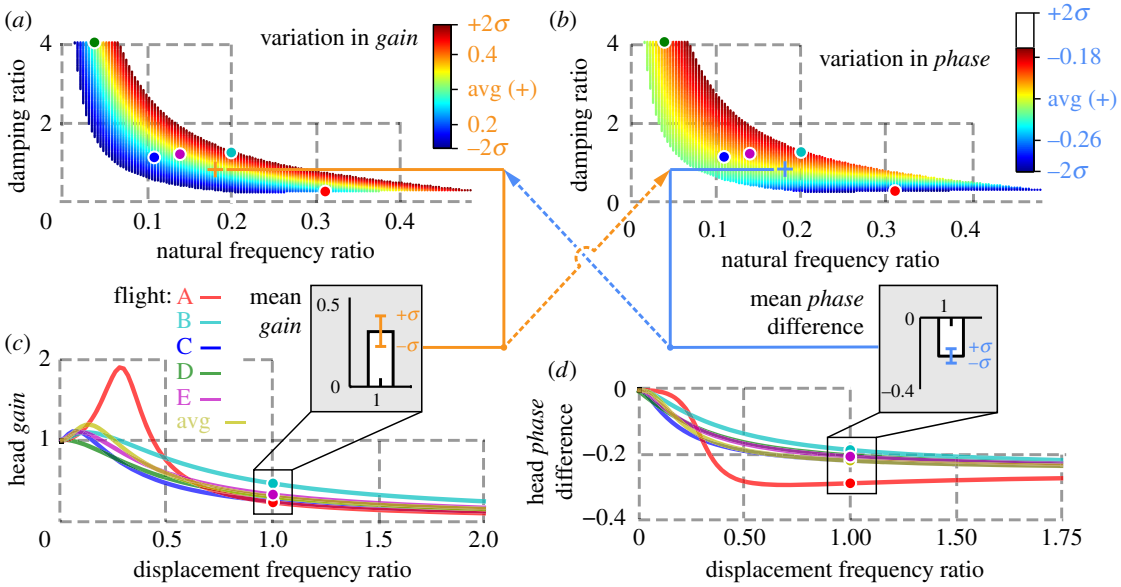

Figure 2. The different frequency and damping ratios for the five flights are connected in parameter space and give similar performance at the wingbeat frequency (displacement frequency ratio = 1). (*a*,*b*) Black dots indicate the predicted values for gain and phase at the wingbeat frequency, respectively, based on the calculated minimal r.m.s.e. damping and natural frequency ratios for all five flights. The '+' symbol represents the point calculated for the average gain and phase over all five flights (the connecting dashed arrows between the box plots in (*c*,*d*) illustrate this). The colour map range represents $\pm 2\sigma$ variation (σ = standard deviation) in the measured gain values (*a*) and phase values (*b*) shown in inset boxplots: (*c*,*d*) Predicted frequency response for gain (*c*) and phase (*d*, measured in flaps) outside the wingbeat frequency (displacement frequency ratio $\neq$ 1). We used corroborated gain and phase values for the plots, as they are not different from the measured ones (see text).

and ζ combinations best represented each of the five flight traces. Using a parameter sweep, we minimized the r.m.s.e. between simulated and measured head displacement in response to the tracked body displacement (custom MATLAB R2013a script; for all five flights, A–E, r.m.s.e. = 0.24; 0.16; 0.18; 0.24; 0.23, fraction of body displacement amplitude). The characteristic parameters corresponding to average gain and phase are $\omega_n/\omega_{\text{flap}} = 0.18$ and $\zeta = 0.86$, suggesting that the average neck of a whooper swan is near critically damped ($\zeta = 1$), and its natural frequency is about five times slower than the flapping frequency (figure 2*a*,*b*). We evaluated gain and phase response beyond just the flapping frequency (ratio = 1) to determine the robustness of the corroborated neck suspension system to other displacement frequencies, such as those experienced in gusts (figure 2*c*,*d*). We see, in general, a small gain peak at the natural frequency ratio with attenuation at higher frequencies. Flight A is notable for predicting a more pronounced amplification of head motion at the natural frequency, because it is underdamped ($\zeta < 1$). Regardless, each model is a good predictor at frequencies close to the flapping frequency (Kruskal–Wallis test for measured and corroborated values indicates no difference: $p = 0.46$ for gain, $p = 0.35$ for phase). To test performance beyond a calm atmosphere, we need to perturb the system.

3. Robustness of passive head stabilization to perturbations

Two common challenges for head stabilization in birds are carrying additional mass in the beak, such as foodstuff and nesting material, and withstanding atmospheric gusts due to turbulence.

To evaluate the added mass effect, we add a fraction δ so that the effective head mass becomes $(1 + \delta)m$. We find that this additional mass actually slightly improves the gain of the neck suspension system when forced at the wingbeat frequency:

$$|\tilde{G}(\omega = \omega_{\text{flap}})| = \left|\frac{\tilde{\Delta}_{\text{head}}}{\Delta_{\text{body}}}\right| = \frac{\sqrt{1 + (2\zeta/(\omega_n/\omega_{\text{flap}}))^2}}{\sqrt{\left(1 - \left(\sqrt{1+\delta}/(\omega_n/\omega_{\text{flap}})\right)^2\right)^2 + (2\zeta/(\omega_n/\omega_{\text{flap}}))^2}}. \quad (3.1)$$

For example, a 20% increase in effective head mass reduces head gain from 0.31 to 0.26, and a 100% mass increase reduces gain further to 0.156, while head phase difference remains essentially the same (−0.23 and −0.24 flaps, respectively). Because both ζ and ω_n are proportional to $1/\sqrt{m}$, the ratio ζ/ω_n remains unchanged and we thus find that this additional mass actually offers slightly improved gain response when forced at the wingbeat frequency (in terms of the original unperturbed ζ and ω_n).

We evaluate the ability of the passive neck suspension to negate vertical gusts by perturbing the body with a vertical sigmoidal displacement. The resultant body displacement, $\gamma(t)$, as a function of wingbeat time, t, measured in flaps is

$$\gamma(t) = \sin(2\pi t) + \frac{A}{1 + e^{\beta(\phi T/2\pi - t)}},$$

where the first term represents the body oscillation induced by the flapping wings, and the second term is the gust-induced body displacement. A is the total displacement amplitude, β is a measure of gust steepness and ϕ is the phase of the wingbeat at gust onset (the wingbeat period, T, is equal to 1 flap). To interpret the gust intensity, we measure gust displacement amplitude in body amplitudes and gust duration in wingbeats (time from 1 to 99% displacement). The resultant body motion was used to predict the head response

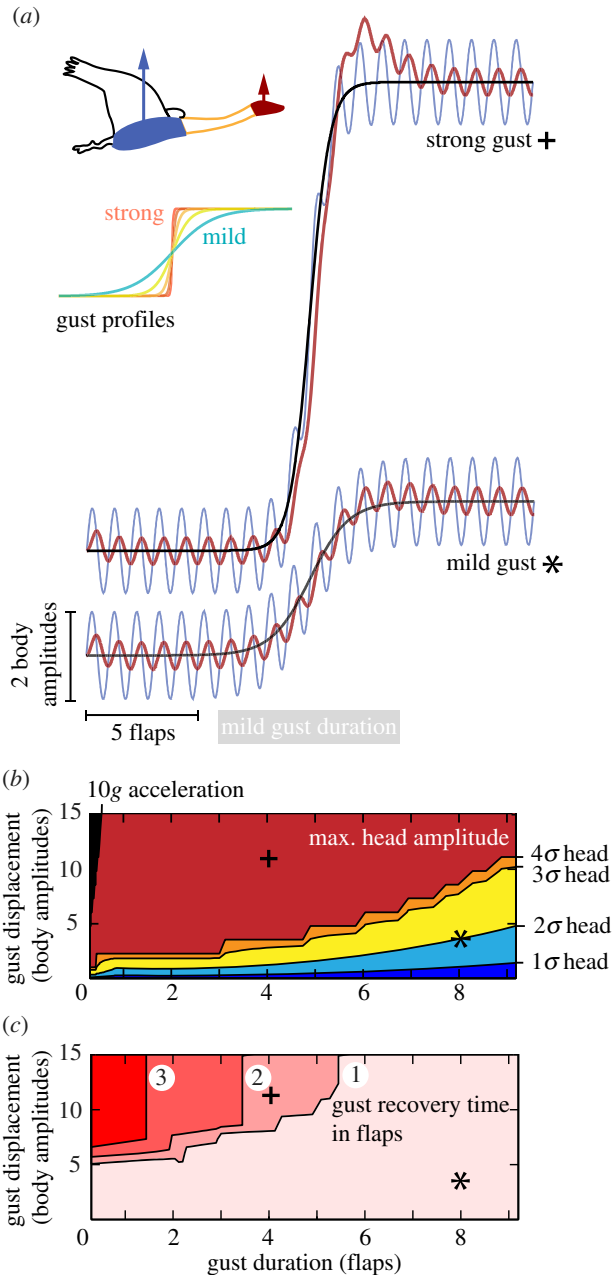

Figure 3. Passive head stabilization is robust to mild gusts that perturb the swan. (*a*) Example of the effect of a mild (asterisk (*) symbol; 3.5 body amplitudes, eight flaps) versus a strong gust (plus (+) symbol; 11.1 body amplitudes, 4.12 flap) on head stabilization. (Head response, red; body oscillation, blue; gust displacement, black; inset shows a range of simulated gusts.) (*b*) The maximal neck amplitude response in a mild gust can stay within 2σ bounds for mild gusts (σ, measured standard deviation of vertical head displacement). Red and black shaded areas indicate physically unreasonable responses that require active avoidance. (*c*) The recovery time after a mild gust, measured in number of flaps needed to return within the measured 2σ range, is less than one wingbeat.

(figure 3*a*) for the whooper swan neck parameters $\omega_n/\omega_{\text{flap}} = 0.18$ and $\zeta = 0.86$ using numerical time-integration (custom MATLAB R2013a script). The wide range of simulated perturbations show that whereas passive head stabilization cannot negate strong gusts (figure 3, plus symbol), it is remarkably effective for negating mild gusts (figure 3, asterisk symbol). During mild gusts, the passive suspension can keep vertical neck and head amplitudes within the $\pm 2\sigma$ *in vivo* range (figure 3*b*). Additionally, the head can recover passively to this $\pm 2\sigma$ *in vivo* amplitude range within one wingbeat after the gust (figure 3*c*). Our simulations show these findings are insensitive to the onset (phase) of gust perturbation within a wingbeat (electronic supplementary material, figure S3).

4. Conclusion and applications

The flight video data and corroborated neck suspension model show that whooper swans can passively attenuate oscillatory body displacements caused by the wingbeat. Passive head stabilization improves with additional mass carried in the beak—and it is robust to mild gusts. Our analysis shows that the compensatory beat-by-beat neck motion of the whooper swan can be replicated with a passive suspension system. Therefore, we hypothesize that swans and other birds can simply tune the stiffness and damping of their neck muscles to stabilize their head and the sensory systems within. Such tuning can be relatively slow and need not occur on a wingbeat to wingbeat timescale. Thus, passive attenuation of harmonic body oscillation due to flapping may enable more effective allocation of neural processing for generating neck motor patterns of more complex visual behaviours such as superfast head saccades [2,15]. To corroborate evidence *in vivo*, further study of the avian cranio-cervical system (positions the head relative to the neck), dorsal system (elevates head and neck), ventral system (depresses head and neck) and thoraco-cervical system (positions the neck relative to the body) is needed [15]. Comparing our passive neck model for whooper swans with models for humans, the swan neck appears to be closer to critically damped when perturbed ($\zeta_{\text{swan}} = 0.86$ versus $\zeta_{\text{human}} = 0.42$–$0.64$, [12]). Unsurprisingly, bird-inspired drones with flapping wings suffer from similar 'wingrock' during flight as the whooper swan. Therefore, designers of flapping drones have focused on aerodynamically inefficient X-wing configurations that vibrate less [16,17]. To test whether a passive neck suspension could resolve this, we built a simple mechanical suspension based on whooper swan parameters, which indeed stabilizes video well (electronic supplementary material, video S2). Future bird-inspired drones with flapping wings may thus combine better efficiency with better imaging using a critically damped passive camera suspension inspired by the whooper swan.

Data accessibility. Data and additional information available at public repository: http://purl.stanford.edu/pw311wn7849.

Competing interests. We declare we have no competing interests.

Funding. This research was supported by ONR MURI grant no. N00014-10-1-0951, HFSP grant no. RGP0003/2013 and a Stanford Bio-X IIP Seed Grant.

References

1. Warrick DR, Bundle MW, Dial KP. 2002 Bird maneuvering flight: blurred bodies, clear heads. *Integr. Comp. Biol.* **42**, 141–148. (doi:10.1093/icb/42.1.141)

2. Kress D, van Bokhorst E, Lentink D. 2015 How lovebirds maneuver rapidly using super-fast head

saccades and image feature stabilization. *PLoS ONE* **10**, e0129287. (doi:10.1371/journal.pone.0129287)

3. Land M. 1999 The roles of head movements in the search and capture strategy of a tern (Aves, Laridae). *J. Comp. Physiol. A* **184**, 265–272. (doi:10.1007/s003590050324)
4. Goller B, Altshuler DL. 2014 Hummingbirds control hovering flight by stabilizing visual motion. *Proc. Natl Acad. Sci. USA* **111**, 18 375–18 380. (doi:10.1073/pnas.1415975111)
5. Ogilvie MA, Wallace DIM. 1975 Field identification of grey geese. *Br. Birds* **68**, 57–67.
6. Katzir G, Schechtman E, Carmi N, Weihs D. 2001 Head stabilization in herons. *J. Comp. Physiol. A Sensory Neural Behav. Physiol*. **187**, 423–432. (doi:10.1007/s003590100210)
7. McArthur KL, Dickman JD. 2011 State-dependent sensorimotor processing: gaze and posture stability during simulated flight in birds. *J. Neurophysiol*. **105**, 1689–1700. (doi:10.1152/jn.00981.2010)
8. Erichsen JT, Hodos W, Evinger C, Bessette BB, Phillips SJ. 1898 Head orientation in pigeons: postural, locomotor and visual determinants. *Brain Behav. Evol*. **33**, 268–278. (doi:10.1159/000115935)
9. Pozzo T, Berthoz A, Lefort L. 1990 Head stabilization during various locomotor tasks in humans. *Exp. Brain Res*. **82**, 97–106. (doi:10.1007/BF00230842)
10. Paddan GS, Griffin MJ. 1988 The transmission of translational seat vibration to the head—I. Vertical seat vibration. *J. Biomech*. **21**, 191–197. (doi:10.1016/0021-9290(88)90169-8)
11. Fard M, Ishihara T, Inooka H. 2004 Identification of the head–neck complex in response to trunk horizontal vibration. *Biol. Cybern*. **90**, 418–426. (doi:10.1007/s00422-004-0489-z)
12. Tangorra JL, Jones LA, Hunter IW. 2003 Dynamics of the human head–neck system in the horizontal plane: joint properties with respect to a static torque. *Annu. Biomed. Eng*. **31**, 606–620. (doi:10.1114/1.1566772)
13. Hedrick TL. 2008 Software techniques for two- and three-dimensional kinematic measurements of biological and biomimetic systems. *Bioinspir. Biomim*. **3**, 034001. (doi:10.1088/1748-3182/3/3/034001)
14. Alexander RM. 2003 *Principles of animal locomotion*. Princeton, NJ: Princeton University Press.
15. Zweers G, Bout R, Heidweiller J. 1994 Motor organization of the avian head–neck system. In *Perception and motor control in birds* (eds MN Davies, PR Green), p. 354. Berlin, Germany: Springer.
16. Lentink D, Jongerius SR, Bradshaw NL. 2009 The scalable design of flapping micro-air vehicles inspired by insect flight. In *Flying insects and robots* (eds D Floreano, J-C Zufferey, MV Srinivasan, C Ellington), pp. 185–205. Berlin, Germany: Springer. (doi:10.1007/978-3-540-89393-6_14)
17. Tay WB, van Oudheusden BW, Bijl H. 2014 Numerical simulation of X-wing type biplane flapping wings in 3D using the immersed boundary method. *Bioinspir. Biomim*. **9**, 036001. (doi:10.1088/1748-3182/9/3/036001)